LONGITUDINAL MEASUREMENTS AND SIMULATIONS OF STRETCHED BUNCHES IN THE NSLS VUV RING

N. Towne*, National Synchrotron Light Source
Brookhaven National Laboratory, Bldg. 725B, Upton, NY 11973-5000†

Abstract

Certain longitudinal instabilities in the stretched bunches of the National Synchrotron Light Source Vacuum Ultra-Violet ring are described and simulated using a code for the integration of the Vlasov-Fokker-Planck equation (these proceedings). Results for the microwave instability driven by broadband impedance, instability driven by high-Q radio-frequency modes, and response functions in stretched bunches, are compared with measurements from the ring.

1 INTRODUCTION

The saturation and relaxation of longitudinal instabilities in storage rings driven by both broad-band impedances [1, 2, 3, 4] and high-Q impedances [5] have been studied in recent years. These studies have shed considerable light on the limiting of these instabilities and highlighted the limits of linearized treatments of coherent modes and frequencies in bunched beams. But nonlinear behavior of bunched beams in which synchrotron frequency spread is introduced for Landau damping and lifetime improvement [6] has been less well studied [7]. This paper describes the results of simulations using the Vlasov-Fokker-Planck (VFP) equation for non-Gaussian bunches and comparisons with observations in the National Synchrotron Light Source (NSLS) vacuum ultraviolet (VUV) ring (Sec. 3). The code used is based on the method of Warnock and Ellison [1] but extended to accommodate non-harmonic radio-frequency (rf) potentials and ring impedances containing high-Q impedances as well as a broad-band impedance [8]. Results of calculations of longitudinal beam response functions (BRFs), which are response functions that include the influence of the beam acting back upon itself through the ring impedance, are also presented (Sec. 2).

2 RESPONSE FUNCTIONS

The beam's response to the *total* longitudinal voltage in the ring is the beam transfer function (BTF) G_{mn} [9, 10]. The parameters m and n are the harmonics about which the beam is sensed and excited respectively. This function is easily measured at low current where the beam-induced voltage of both the broad-band impedance and high-Q impedances are small. One can also measure it at higher currents about a non-rf harmonic in a multi-bunch full

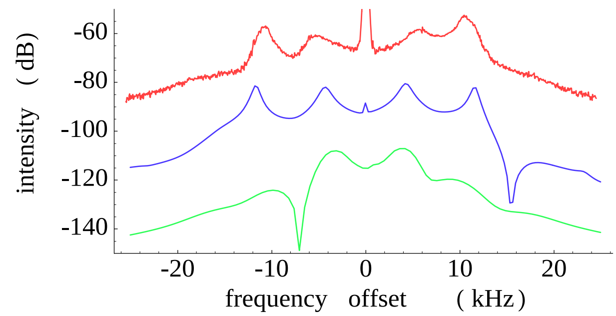

Figure 1: Measured (top trace) and simulated beam response functions T_{mn} in the VUV ring. The top trace was $T_{54\,54}$ taken from a 205-mA seven-bunch beam while the middle and lower traces were single-bunch simulations of $T_{55\,55}$ at 500 mA and 11 mA respectively. Only rf-cavity high-Q impedances, which were realistically tuned for beam-loading compensation, were included in the 500-mA simulation while a broad-band impedance was in the second. The rf potential and other ring parameters are given Table 1. The vertical scale is arbitrary .

where the voltages induced by the broad-band impedance is still small and cavity accelerating mode impedances do not participate in the response functions (higher-order modes can still influence the measurement).

The beam response function (BRF) T_{mn} is the response of the beam to an *external* excitation; it includes the beam acting back upon itself through the ring impedances. It is of considerable interest to predict BRFs because they contain information about the ring impedance. In particular, BRFs at frequencies surrounding bunch harmonics at high total current contain formation about accelerating-mode impedances and BRFs at high single-bunch current contain information about broad-band impedances.

This section describes how accelerating-mode impedances influence BRFs in the NSLS VUV ring. BRFs were measured by sweeping the frequency of an rf voltage applied through a strip line and sensing the synchrotron sidebands through button pickups. The frequency range is ±25 kHz about the 54th revolution line and the fill is seven of nine bunches. Simulations by the method described in Ref. [8] using VUV-ring parameters were also done. Figure 1 shows a comparison between these response functions.

The simulation of the third trace of Fig. 1 has a broad-band impedance and a current sufficiently small that it does not significantly affect the response function. $T_{mn} \simeq G_{mn}$

* Email: towne@bnl.gov
† Work performed under the auspices of the U.S. Department of Energy, under contract DE-AC02-76CH00016.

in this case. It is in close agreement with VUV measurements at low current as well as with calculations of G_{mn} using Shaposhnikova's methods [9] and the new method described in Ref. [11]. The BTF has the characteristic lobed structure whose lobes correspond to the terms of the series decomposition of G_{mn} into a sum over the synchrotron harmonics [12]. It is also in close agreement with BRF measurements about non-rf harmonics of higher-current multibunch beams, response functions that are not sensitive to the accelerating modes of the rf cavities.

The beam's response about bunch harmonics (top trace of Fig. 1) contains peaks at about 5- and 12-kHz offsets. Since these peaks are absent when there are no high-Q rf modes, the main- and harmonic-cavity fundamental rf modes are responsible for these peaks. The frequencies of these peaks are relatively insensitive to current although there are trends in their damping rates. These observations were confirmed in response-function calculations where the ring impedance includes the main- and harmonic-cavity rf-mode impedances (second trace of Fig. 1). The multipole orders of the coherent motion associated with the 5-kHz and 12-kHz peaks were established by computing the time dependence of the first- and second-order moments of the bunch and comparing their intensities. The results showed that the 5- and 12-kHz peaks are due primarily to dipole and quadrupole oscillations although there is considerable mode coupling in both cases. These observations are consistent with the calculations of T.-S. Wang and Bosch [13, 7] showing that dipole-quadrupole mode coupling is significant in stretched bunches. Progressively stretching the bunch in machine tests also shows continuity between the short-bunch quadrupole resonance and the 12-kHz peak in stretched bunches.

At low current, simulations predict that the quadrupole mode becomes unstable at 200 mA and below. In contrast, Fig. 1, which was taken from the VUV ring at 205 mA, shows that the quadrupole mode is rather well damped at that current. So the simulations and predictions are not in close agreement; fine tuning of the cavity impedances may be needed to make up some of the discrepancy. Nevertheless, the identities of the two peaks as dipole and quadrupole modes respectively remain intact over that current range and beyond. These results resolved the long-standing question regarding the origin of the 5- and 12-kHz peaks in beam response functions and noise sidebands and provided some information about the degree of mode coupling involved.

3 INSTABILITIES

Simulations of stretched bunches in the VUV ring at lower currents predict instability depending in detail on the high-Q accelerating-mode impedances of the rf cavities. This instability is predicted by other authors [13, 7]. The simulations show that the bunch distribution, when the instability is not too intense, turns in the phase space with a two-fold symmetry. Depending on conditions, the distribution may rotate steadily, have regular bursts, or irregular bursts. At 150 mA current, given machine conditions the same as in Sec. 2, the distribution undergoes a steady rotation with a concentration of particles in the center with two opposite lobes. Figure 2 shows the bunch distribution in phase space looking from the low-energy side of the bunch with the leading edge to the right. Simulated synchrotron sidebands show sharp lines at harmonics of 12 kHz.

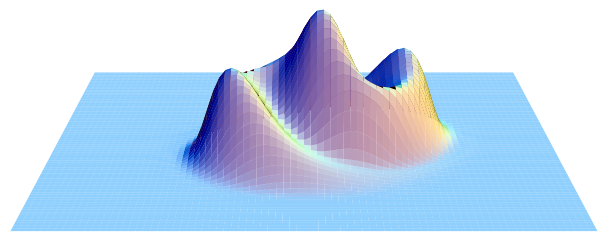

Figure 2: Simulated phase-space distribution of a 150-mA fully stretched unstable bunch after the oscillations have steadied. The ring impedance consists of main- and harmonic-cavity fundamental rf modes with tunes realistically adjusted for beam-loading compensation. There is no relaxation cycle. Particle energy is from front to back and phase is left to right. The leading edge of the bunch is to the right. Machine parameters are given in Table 1.

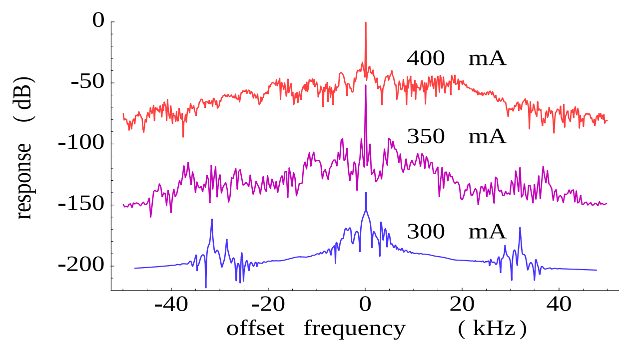

Figure 3: Spectra of simulated microwave-unstable bunches in the NSLS VUV ring at three beam currents. The ring impedance is that of a Q=1 resonator with $|Z_n/n| = 2.3\ \Omega$ and resonant frequency 1.8 GHz. Successive traces are displaced vertically 50 dB. Machine parameters are given in Table 1.

At 300 mA with high-Q rf modes alone, however, the bunch is stable in simulation. Given the same 300-mA current but with only a model broad-band impedance that consists of a $Q = 1$ resonator with $|Z_n|/n = 2.3\Omega$ and resonant frequency 1.8 kHz present in the ring impedance, the bunch is microwave unstable but is without bursting mode. There is only steady bunch lengthening. Additional current brings the bunch into the turbulent regime and the bursting mode of behavior. A current of 350 mA is sufficient to do this (Fig. 3).

When high-Q and broad-band impedances are combined

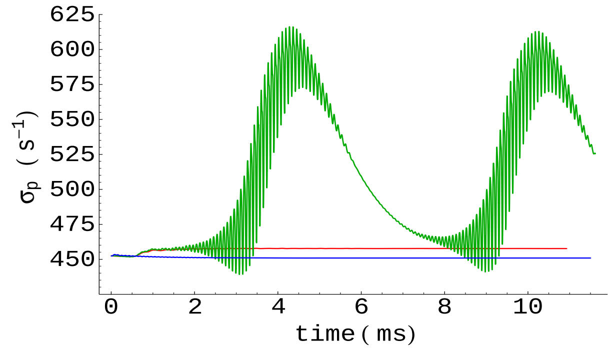

Figure 4: Simulated energy spreads of three 300-mA fully stretched bunches that differ in the ring impedances in which they propagate. The ring impedances are: main- and harmonic-cavity fundamental rf modes only (blue, lower trace); broad-band impedance consisting of a Q=1 resonator with $|Z_n/n| = 2.3\ \Omega$ and resonant frequency 1.8 GHz only (red, middle trace); and broad-band impedance and high-Q rf modes combined (green, upper trace). The tunes of the rf modes are realistically adjusted for beam-loading compensation. Machine parameters are given in Table 1.

at a current of 300 mA, the simulated bunch is also tipped into the bursting-mode regime. Figure 18 shows energy spread against time from three simulations, one with only the high-Q impedances of the rf cavities (bottom, blue), one with only the broad-band impedance (middle, red), and a third with both (upper, green). The plot of the energy spread of this bursting-mode instability of the last case has an appearance very similar to that of a short-bunch simulation of Ref. [4]. The spectrum of the steady-state condition of the lowest trace has sharp lines; the extended sidebands arise from the initial transient associated with the start of the simulation. The approximation that the bunch appears to the microwave radiation to be a coasting beam is unusually good for a stretched bunch. This permits an estimate of the offset of the sharply peaked sidebands to be simply derived; it is $\omega = \sqrt{2}\,\alpha\,\sigma_\epsilon\,\omega_\lambda$, where ω_λ is the frequency of the microwave radiation and other parameters are given in Table 1. The derivation is not given here. These sidebands have not been observed at any offset in the VUV ring.

4 CONCLUSION

This paper touched on a few characteristics of stretched bunches predicted by time-domain simulations. The comparison of simulated and measured beam response functions provides an understanding of the origin of peaks in the response functions in terms of the rf-cavity accelerating-mode impedances. Their multipole orders are also illuminated. The simulation of high-Q rf-mode driven instabilities, broad-band-impedance driven instabilities, and their combination show bunch lengthening through the microwave instability and a bursting mode when present in combination.

5 ACKNOWLEDGMENTS

The author thanks Jiunn-Ming Wang, Sam Krinsky, and Bob Bosch for helpful discussions.

Table 1: Storage ring and main- and harmonic-cavity parameters (separated by a forward slash), symbols, and VUV-ring values.

parameter	symbol	value
synchronous energy	E_0	800 MeV
energy loss per turn	U_0	20.4 keV
momentum compaction	α	0.0245
revolution frequency	ω_0	$2\pi \times 5.876$ MHz
radiation damping rate		1/7 ms
fractional energy spread	σ_ϵ	5×10^{-4}
rf harmonic numbers	h	9/36
rf peak voltages	V_h	80/19.7 kV
rf phases	ψ_h	$74.2^\circ/-90^\circ$
rf cavity impedances	R_h	435/100 kΩ
loaded quality factors	Q_h	6800/3360

6 REFERENCES

[1] R. Warnock and J. Ellison, in *The 2nd ICFA Advanced Accelerator Workshop on the Physics of High Brightness Beams*, University of California, Los Angeles, November 9-12, 1999 (World Scientific, Singapore, 1999).

[2] B. V. Podobedov, *Saw-tooth Instability Studies at the Stanford Linear Collider Damping Rings*, Ph.D. thesis, Stanford University, Stanford Linear Accelerator Center, Stanford, CA 94309 (1999).

[3] M. Migliorati, L. Palumbo, G. Dattoli, and L. Mezi, Nucl. Instrum. Methods **A437**, 134 (1999).

[4] R. Warnock, K. Bane, and J. Ellison, in *7th European Particle Accelerator Conference* (Vienna, Austria, 2000), Stanford Linear Accelerator Center Report No. SLAC-PUB-8494.

[5] C. Limborg and J. Sebek, Phys. Rev. **E60**, 4823 (1999).

[6] R. Biscardi, S. L. Kramer, and G. Ramirez, Nucl. Instrum. Methods **A366**, 26 (1995).

[7] R. Bosch, *Robinson Instabilities with a Higher Harmonic Cavity* (2001), in preparation.

[8] N. Towne, in *2001 IEEE Particle Accelerator Conference* (ANL and IEEE, 2001).

[9] E. N. Shaposhnikova, *Bunched Beam Transfer Matrices in Single and Double RF Systems*, Tech. Rep. SL-94-19-RF, CERN - SL Division, Geneva, Switzerland (1994).

[10] S. Krinsky and J. M. Wang, Part. Accel. **17**, 109 (1985).

[11] N. Towne, in *2001 IEEE Particle Accelerator Conference* (ANL and IEEE, 2001).

[12] A. N. Lebedev, At. Energ. **25**(2), 100 (1968), [Sov. J. At. Energy, Vol. 25, p. 851-6 (1968)].

[13] T. S. F. Wang, Part. Accel. **34**, 105 (1990).